

SURFACE CHEMISTRY OF MESOPOROUS CARBON MOLECULAR SIEVES

H. Darmstadt¹, C. Roy¹, S. Kaliaguine¹, S.J. Choi² and R. Ryoo²

¹ *Chemical Engineering Department, Laval University*

Québec, Qc, G1K 7P4, Canada, E-mail: darmstad@gch.ulaval.ca

² *Department of Chemistry (School of Molecular Science – BK21), Korea Advanced Institute of Science and Technology, Taejon, 305-701, Korea, E-mail: rroyo@mail.kaist.ac.kr*

Introduction

Many industrial processes involve the adsorption and catalytic conversion of large hydrocarbons. The ideal carbonaceous adsorbent or catalyst support for these applications should have pores somewhat wider than the dimensions of the hydrocarbons (*i.e.* some ten Angstroms). Furthermore, the pore size distribution should be narrow and the volume of other pores (especially micropores) should be small in order to favour the transport and adsorption of the large hydrocarbons over other (especially smaller) hydrocarbons. Unfortunately, these requirements are not fulfilled by the widely used activated carbons. However, mesoporous carbon molecular sieves with the desired properties can be produced by pyrolysis/carbonisation of hydrocarbons adsorbed in a suitable silica matrix. In a second step of the synthesis, the silica matrix is dissolved in either sodium hydroxide or hydrofluoric acid [1,2].

In a previous investigation, the pore structure of carbon sieves synthesised in two silica matrices was studied by

low-pressure nitrogen adsorption [3]. In addition to the pore structure, the surface chemistry is also very important for the adsorption behaviour. Therefore, in the present work, the surface chemistry of the carbon sieves was studied in detail by two spectroscopic methods: electron spectroscopy for chemical analysis (ESCA) and static secondary ion mass spectroscopy (SIMS). The combination of these two techniques is attractive since different portions of the surface are studied. Static SIMS only probes the first atomic layer, whereas by ESCA, information on the surface chemistry up to a depth of approximately 50Å is obtained. Thus, by ESCA, in addition to the surface, surface-near regions are also studied.

It should be mentioned, that the largest portion of the surface of the carbon sieves is located in meso- and micropores. The outer surface studied by ESCA and SIMS represents therefore only a small portion of the total surface. However, it was possible to obtain information on the graphitic order of the mesopore surface from low-pressure nitrogen adsorption data [3]. The comparison of the sur-

Table 1, Synthesis parameters of the mesoporous carbon molecular sieves

Carbon sieves produced in a MCM-48 matrix				Carbon sieves produced in a SBA-15 matrix			
Sample	Temperature [°C]		Solvent for the matrix	Sample	Temperature [°C]		Solvent for the matrix
	Pyrolysis	Post-pyrolysis heat-treatment			Pyrolysis	Post-pyrolysis heat-treatment	
CMK-1F(A)	700	-	HF	CMK-3F(A)	700	-	HF
CMK-1F(B)	900	-	HF	CMK-3F(B)	900	-	HF
CMK-1F(C)	900	1100 ^a	HF	CMK-3F(C)	900	1100 ^a	HF
CMK-1F(D)	1100	-	HF	CMK-3F(D)	900	1300 ^b	HF
CMK-1F(E)	900	1300 ^b	HF	CMK-3F(E)	900	1600 ^b	HF
CMK-1F(F)	900	1600 ^b	HF				
CMK-1Na(A)	700	-	NaOH	CMK-3Na(A)	700	-	NaOH
CMK-1Na(B)	900	-	NaOH	CMK-3Na(B)	900	-	NaOH
CMK-1Na(C)	900	1100 ^a	NaOH	CMK-3Na(C)	1100	-	NaOH
CMK-1Na(D)	900	1300 ^b	NaOH				
CMK-1Na(E)	900	1600 ^b	NaOH				

^a Under vacuum

^b Under nitrogen

face spectroscopy and gas adsorption results allows one to estimate how representative the surface spectroscopic results are for the entire surface of the carbon sieves.

The carbon sieves were produced in MCM-48 and SBA-15 silica matrices, respectively, at different pyrolysis and post-pyrolysis heat-treatment temperatures. An important difference between the two matrices is that in the case of SBA-15 the carbon sieves are a replica of the matrix, whereas the structure of carbon sieves produced in MCM-48 changes upon removal of the matrix [4].

Experimental Details

Materials

The carbon sieves were produced by pyrolysis of sucrose adsorbed in a MCM-48 and a SBA-15 silica matrix, respectively. Different pyrolysis experiments were performed at temperatures ranging from 700 to 1100 °C. Then, the carbon sieves were liberated by dissolving the silica matrix in either hydrofluoric acid or sodium hydroxide solution. Some samples were subsequently heat-treated at temperatures ranging from 1100 to 1600 °C. The synthesis conditions of the mesoporous carbons are summarised in Table 1. Detailed information on the synthesis of the MCM-48 [5] and the SBA-15 [4] silica matrices as well on the synthesis of the carbon sieves [4,6] can be found elsewhere.

Electron spectroscopy for chemical analysis (ESCA)

An ESCALAB MK II spectrometer (VG Scientific, East Grinstead, UK) equipped with a Microlab system from Vacuum Generators (Hastings, UK) with non-monochromatized Mg K_{α} radiation was used for the ESCA experiments. The binding energy scale was corrected by referring the C_{1s} peak in the C_{1s} signal at 284.4 eV. However, the corrections made were smaller than 0.05 eV. The pressure during the experiments was lower than 10^{-9} mbar. After removal of satellites and of a non-linear background from the spectra, a mixed Gaussian-Lorentzian product function was used to describe the shape of the peaks [7]:

$$I = \frac{I_0}{\left(1 + \frac{m(x - x_0)^2}{b^2}\right) \exp\left(\frac{(1 - m) \ln 2 (x - x_0)^2}{b^2}\right)} \quad (1)$$

where I is the intensity, I_0 is the maximum peak height, x is the binding energy, x_0 is the binding energy at the peak centre, b is a parameter for the peak width that is nearly half the full width at half maximum (FWHM) and m is the Gauss-Lorentz mixing ratio; with $m = 0$ a pure Gaussian curve is obtained, whereas $m = 1$ gives a pure Lorentzian curve.

The C_{1s} peaks of the carbon spectra had an asymmetric shape. Their shape was described by an exponential tail, added to the high binding energy side of the peak [7]:

$$I' = I + (1 - I)(1 - TMR)e^{-ETR(x - x_0)} \quad (2)$$

where I' is the intensity of the asymmetric peak, TMR is the tail mixing ratio and ETR is the exponential tail ratio.

A program developed at Université Laval was used to calculate the relative sensitivity factors for the determination of the elemental composition on the surface. This program considers the Scofield photo-ionisation cross-sections, angular asymmetry factors, transmissions and the electron mean free path in the calculation. The surface area probed by ESCA was approximately 5 mm².

Secondary Ion Mass Spectroscopy (SIMS)

A Vacuum Generator SIMSLAB equipped with a Wien-filtered AG61 ionisation ion gun and an MM12-12S quadrupole mass spectrometer was used for the SIMS experiments. The SIMS spectra were recorded using Ar⁺ ions with a current density smaller than 1 nA / cm² and an energy of 1 keV at a pressure lower than 10^{-7} Pa. The total ion dose after recording the positive and negative SIMS spectra at these settings was lower than $0.5 \cdot 10^{13}$ ions/cm². It was shown previously that below an ion dose of $1.0 \cdot 10^{13}$ ions/cm² no significant degradation of carbonaceous surfaces takes place [8]. Thus, in the present work true static SIMS spectra were obtained. The argon ion beam diameter was 100 μm, the scanned surface area was 16 mm² and the angles of incidence and emission were 45 and 0° with respect to the surface normal, respectively. The mass resolution was better than 0.6 atomic mass units (amu) at 5 % peak height. The powdered carbon sieves were placed in stainless steel sample holders where they were only held by gravity.

Results and Discussion

Surface Composition determined by ESCA

The survey spectra of the carbon sieves showed in addition to peaks of carbon and oxygen only small signals of silicon and fluorine. As an example, the survey spectrum of carbon sieve CMK-1F(C) is presented in Fig. 1. On the carbon sieves liberated from the silica matrix with sodium hy-

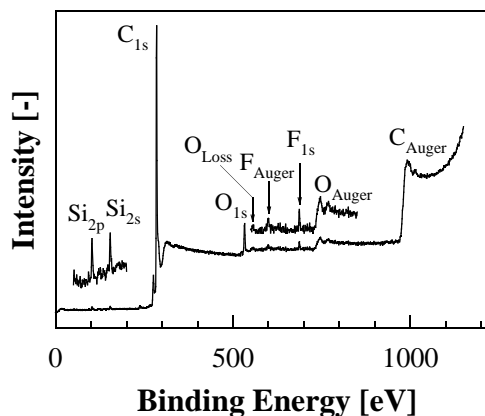


Fig. 1 ESCA Survey spectrum, sample CMK-1F(C)

Table 2, Elemental surface composition

Sample	Element [atom %]			
	C	O	Si	F
CMK-1F(A)	95.4	4.1	0.2	0.3
CMK-1F(B)	96.3	2.9	0.3	0.5
CMK-1F(C)	93.6	4.6	1.1	0.7
CMK-1F(D)	94.2	4.4	0.6	0.8
CMK-1F(E)	99.0	0.7	0.3	^a
CMK-1F(F)	99.1	0.8	0.1	^a
CMK-1Na(A)	94.8	5.2	^a	^a
CMK-1Na(B)	95.8	4.2	0.2	^a
CMK-1Na(C)	95.4	3.4	1.2	^a
CMK-1Na(D)	97.5	1.5	1.0	^a
CMK-1Na(E)	99.7	0.3	^a	^a
CMK-3F(A)	96.5	3.5	^a	^a
CMK-3F(B)	97.0	2.4	0.3	0.3
CMK-3F(C)	98.2	1.5	0.3	^a
CMK-3F(D)	99.2	0.7	0.1	^a
CMK-3F(E)	100.0	^a	^a	^a
CMK-3Na(A)	95.9	4.1	^a	^a
CMK-3Na(B)	96.8	2.9	0.3	^a
CMK-3Na(C)	97.1	2.5	0.4	^a

^a Below the detection limit at reasonable acquisition time

droxide solution (series CMK-1Na and CMK-3Na) no sodium was found. Fluorine was only detected on carbon sieves liberated by dissolving the silica matrix in hydrofluoric acid (series CMK-1F and CMK-3F), indicating that the fluorine originated from the hydrofluoric acid. It should be recalled that hydrogen, which is most probably present on the carbon surface, cannot be detected by ESCA.

The most important element on the surface was carbon. Its concentration ranged from 93.6 to 100.0 atom % (Tab. 2). With increasing pyrolysis or post-pyrolysis heat treatment temperature the surface concentration of non-carbon elements decreased. This decrease can be explained by removal of thermally unstable surface functional groups (*e.g.* -OH and -COOH). On the surface of one of the samples heat-treated at 1600 °C (CMK-3F(E)) no elements other than carbon were found.

The low oxygen concentration on the surface of the heat-treated carbon sieves is an indication that the surface of these samples was well ordered with no or only a very small concentration of defects. This becomes evident by comparison with other carbonaceous solids. For activated carbons it was observed that an important portion of the oxygen lost upon

heat-treatment was re-adsorbed as soon as the heat-treated activated carbon came in contact with the atmosphere [9]. It was assumed that surface defects were created during removal of the oxygen. These defects did not "heal" during the heat-treatment and acted as "active" sites for the re-adsorption of oxygen. In the present investigation, the heat-treated carbon sieves were in contact with the atmosphere for a considerable period of time prior to the spectroscopic characterisation. The low surface oxygen concentration on the heat-treated carbon sieves indicates, therefore, that there was only a small concentration of defects on the surface of the heat-treated carbon sieves, which could react with atmospheric oxygen.

ESCA Silicon spectra

The silicon detail spectra were recorded for two carbon sieves (samples CMK-1F(B) and CMK-1F(C)). These spectra showed a doublet with a binding energy (BE) of approximately 102.7 eV for the 2p_{3/2} peak (Fig. 2). This BE is typical for silicon atoms in silicates and silica [10]. The BE of silicon atoms with bonds to carbon atoms is considerably lower (101.0 eV, [10]) and no indication for a peak at this BE was found in the spectra. It can therefore be concluded that small quantities of non-dissolved silica were left on the surface of the carbon sieves, regardless if the dissolution was performed with hydrofluoric acid or with sodium hydroxide.

ESCA Fluorine spectra

On the surface of some carbon sieves, liberated from the matrix by hydrofluoric acid, fluorine was found. The fluorine spectra showed a peak with a BE of approximately 687.0 eV (Fig. 3). Peaks with such a BE were also observed in the spectra of fluorinated carbon blacks [11]. The BE of inorganic fluorides is considerably lower (~

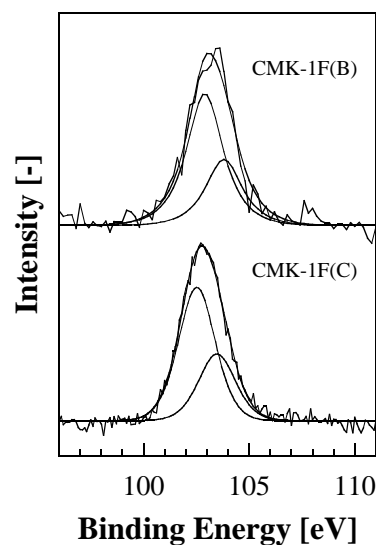


Fig. 2 ESCA Silicon 2p spectra, samples CMK-1F(B) and CMK-1F(C); normalised to the same height

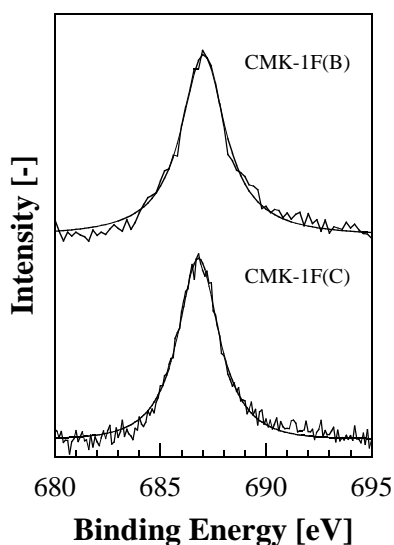


Fig. 3 ESCA Fluorine 1s spectra, samples CMK-1F(B) and CMK-1F(C); normalised to the same height

684.0 eV) [10]. It seems, therefore, likely that during dissolution of the silica framework with hydrofluoric acid, carbon-fluorine groups were formed on the surface of some carbon sieves. Surface fluorine concentrations of up to 0.8 atom % were found (Tab. 2). The quantification of elements in such a small concentration by ESCA contains some experimental uncertainty. However, even when this is taken into account, the surface fluorine concentration on the carbon sieves depended on the silica matrix used for their synthesis. Carbon sieves formed in MCM-48 contained more fluorine on the surface as compared to samples formed in SBA-15. This might be due to a different reactivity of the silica matrix with the hydrofluoric acid.

ESCA Carbon spectra

The carbon spectra were fitted to six peaks: a peak for carbon atoms with bonds to carbon and/or hydrogen atoms (C_1 , BE = 284.4 eV [12,13]); to three peaks for carbon atoms with one, two and three bonds to oxygen atoms (C_2 , C_3 , C_4 ; C-OH, C=O, COOH, BE = 285.9, 287.4 and 288.9 eV [12, 13]) and to two $\pi \rightarrow \pi^*$ peaks (C_5 , C_6 , BE = 290.4 and 294.4 eV, [14]). The C_3 peak also contains a contribution from carbon atoms with one bond to fluorine [11]. The full width at half maximum (FWHM) of the C_1 peak was 1.0-1.2 eV, 2.0 ± 0.2 eV for the C_2 - C_4 peaks and $3.3 \text{ eV} \pm 0.2 \text{ eV}$ for the C_5 and C_6 peaks. The C_1 peak had an asymmetrical shape, whereas the other peaks were symmetrical (Figs. 4a and 4b).

The asymmetry of the C_1 peak obtained by the fitting routine is strongly correlated to the areas of the peaks assigned to carbon – oxygen and carbon – fluorine groups (C_2 - C_4). The concentration of these groups depends of course on the surface concentration of oxygen and fluorine. It is therefore possible to add the following constraint to the fitting

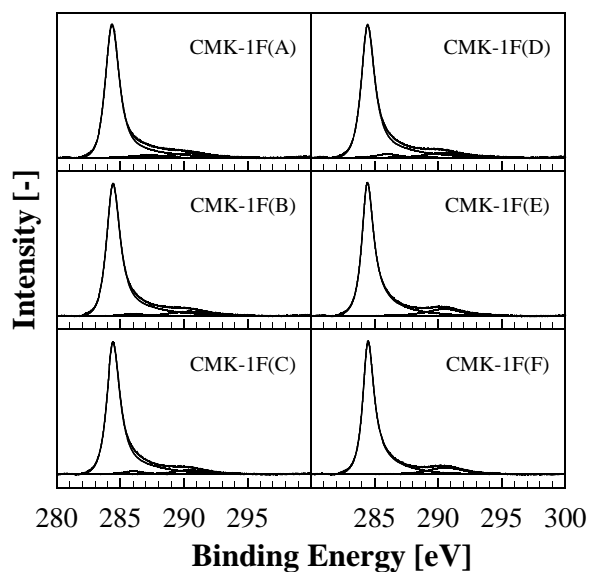


Fig. 4a ESCA Carbon 1s spectra, samples CMK-1F(A) to CMK-1F(F); normalised to the same height

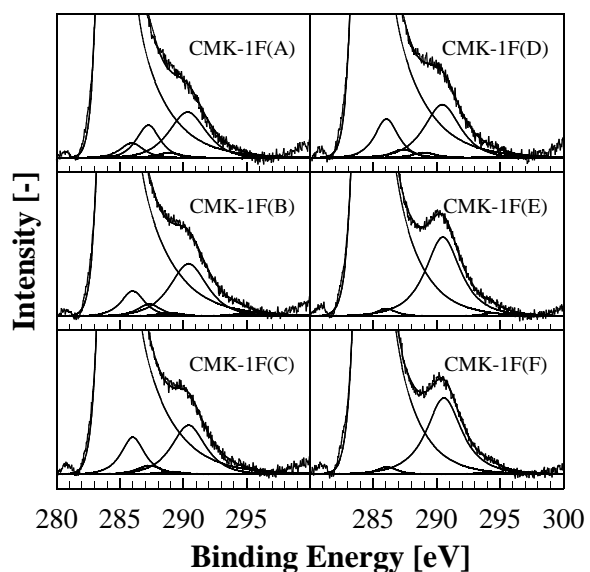


Fig. 4b ESCA Carbon 1s spectra, samples CMK-1F(A) to CMK-1F(F); enlarged to 10 % of maximum height

procedure, which links the area of these peaks to the surface concentration of organic oxygen and fluorine:

$$\frac{\text{Area } C_2 \text{ peak} + \text{Area } C_3 \text{ peak} + 2 \cdot \text{Area } C_4 \text{ peak}}{\text{Total area of the carbon signal}} = \frac{\text{Conc. oxygen} + \text{Conc. fluorine}}{\text{Conc. carbon}} \quad (3)$$

The area of the C_4 peak is multiplied by a factor of two because this peak was assigned to $-\text{COOH}$ groups, where one carbon atom is bonded to two oxygen atoms. Since the es-

cape depths of carbon, oxygen and fluorine are different, it has to be assumed that no concentration gradient exists in the volume probed by ESCA.

All carbon spectra were dominated by an intense, asymmetrical C_1 and a smaller $\pi \rightarrow \pi^*$ (C_5) peak. Such spectra are typical for carbonaceous samples with a graphite-like, polyaromatic surface such as carbon blacks [15] and carbon fibres [12,13]. There were small, but significant differences between the carbon spectra. Important information on the polyaromatic character of a carbon surface can be obtained from different peak parameters [16]. With increasing polyaromatic character, the relative area of the $\pi \rightarrow \pi^*$ peak (C_5) increases [17], the C_1 peak becomes more asymmetrical [18] and its FWHM decreases [19]. In the present work, all these parameters were used to describe the polyaromatic character of the carbon sieve surface. The determination of the area of the $\pi \rightarrow \pi^*$ peak and the FWHM of the C_1 peak is straightforward, whereas there are several possibilities to describe the asymmetry of the C_1 peak [12]. In the present work, the asymmetry of this peak was described by the ratio of the peak area on the high and low binding energy side of the peak maximum (A_H/A_L). A symmetrical peak has an A_H/A_L value of 1, whereas asymmetrical peaks have larger A_H/A_L values. The treatment temperature had a pronounced effect on the carbon spectra. For the samples of the CMK-1F series it can easily be seen

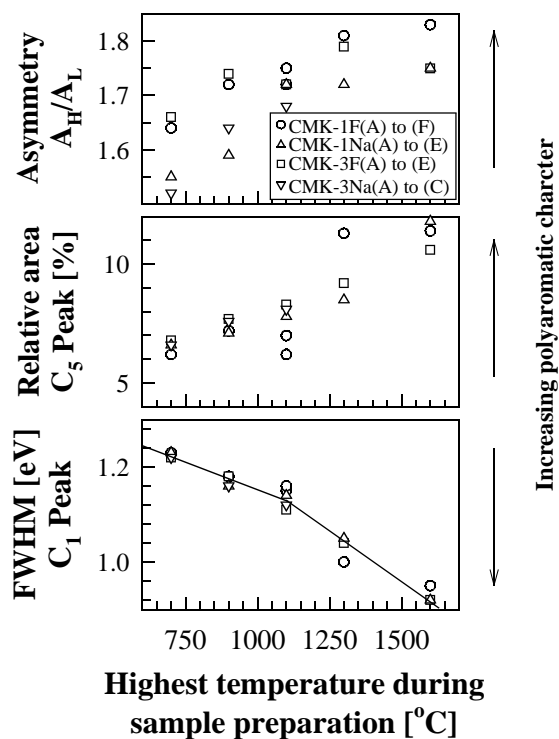


Fig. 5 Polyaromatic character of the surface as a function of the temperature during sample preparation

Table 3, ESCA carbon spectra; peak area and fit parameter of the C_1 peak

Sample	Relative peak area [%]						Parameter of the C_1 peak	
	C_1 C-C	C_2 C-OH	C_3 C=O	C_4 COOH	C_5 $\pi \rightarrow \pi^*$	C_6 $\pi \rightarrow \pi^*$	Asymmetry A_H/A_L	FWHM [eV]
CMK-1F(A)	89.3	1.3	2.8	0.4	6.2	0.0	1.64	1.23
CMK-1F(B)	89.2	2.2	1.0	0.3	7.2	0.2	1.72	1.18
CMK-1F(C)	89.5	3.3	0.8	0.2	6.2	0.0	1.72	1.15
CMK-1F(D)	88.4	3.3	0.7	0.5	7.0	0.1	1.75	1.16
CMK-1F(E)	87.9	0.6	0.0	0.0	11.3	0.2	1.81	1.00
CMK-1F(F)	87.8	0.6	0.0	0.0	11.4	0.2	1.83	0.95
CMK-1Na(A)	87.6	1.9	3.1	0.7	6.6	0.1	1.55	1.23
CMK-1Na(B)	89.5	2.0	1.1	0.4	7.1	0.0	1.59	1.16
CMK-1Na(C)	90.8	1.2	0.0	0.2	7.8	0.0	1.72	1.14
CMK-1Na(D)	90.6	0.6	0.0	0.0	8.5	0.3	1.72	1.05
CMK-1Na(E)	87.2	0.6	0.0	0.0	11.8	0.4	1.75	0.92
CMK-3F(A)	88.8	1.3	2.5	0.3	6.8	0.3	1.66	1.22
CMK-3F(B)	89.2	2.0	0.7	0.1	7.7	0.3	1.74	1.18
CMK-3F(C)	90.5	1.0	0.0	0.0	8.3	0.2	1.72	1.11
CMK-3F(D)	90.0	0.6	0.0	0.0	9.2	0.3	1.79	1.04
CMK-3F(E)	89.2	0.0	0.0	0.0	10.6	0.2	1.75	0.92
CMK-3Na(A)	88.9	1.5	2.5	0.5	6.7	0.0	1.59	1.18
CMK-3Na(B)	89.5	2.0	0.6	0.2	7.2	0.1	1.69	1.17
CMK-3Na(C)	89.5	2.2	0.2	0.0	7.2	0.2	1.55	1.12

that the area of the $\pi \rightarrow \pi^*$ peak increased with increasing heat-treatment temperature (Figs 4a and 4b and Tab. 3). Furthermore, the C_1 peak became narrower and its asymmetry increased (Tab. 3, not easy to see in figures 4a and 4b). All these changes indicate an increasing polyaromatic character of the surface with increasing treatment temperature.

Even if the agreement between the three parameters, which describe the polyaromatic character of the surface, was reasonably good the usefulness of the parameters was not the same. The three parameters are plotted in Figure 5 as a function of the highest temperature used during the synthesis of the carbon sieves. The data indicate some scattering for the peak asymmetry (A_H/A_L value) and the area of the $\pi \rightarrow \pi^*$ peak. The FWHM data, on the other hand, gave a much smoother curve, indicating that for the samples studied the FWHM is the most suitable parameter for the description of the polyaromatic character of the carbon sieve surface.

For a given treatment temperature, the FWHM in the carbon spectra of samples produced in either a MCM-48 or a SBA-15 silica matrix and liberated with either hydrofluoric acid or sodium hydroxide was very similar. This indicates that the polyaromatic character of the carbon surface did not or only very little depend on the silica matrix or on how the silica matrix was dissolved. Since the structure of the silica matrix determines the structure of the carbon sieve, it seems that the structure of the carbon sieve is not very important for the polyaromatic character of its surface. The results indicate that the determining factor was the treatment temperature.

SIMS spectra, negative ions

Static secondary ion mass spectroscopy (SIMS) was used as a second surface spectroscopic method. In the SIMS experiment the sample surface is bombarded with high-energy ions, causing the ejection of ions and neutral species. Which species are ejected depends on the chemical nature of the sample surface. The SIMS spectra of carbonaceous solids with a polyaromatic surface (e.g. carbon blacks [8] and carbon fibres [20]) show intense peaks of C_2H^- and C_2^- ions. These materials consist of graphene layers. The most important contribution to the C_2H^- peak arises from the edge of graphene layers, whereas most of the C_2^- ions originate from the interior of the graphene layers. The ratio of the areas of these two peaks (C_2H^-/C_2^-) is therefore a measure for the inverse size of the graphene layer on the surface of the sample. A low C_2H^-/C_2^- ratio indicates large graphene layers or a high polyaromatic character. This was confirmed by the SIMS spectra of reference compounds. For polycrystalline graphite, the reference compound for a large polyaromatic system, a C_2H^-/C_2^- ratio of 0.25 was found, whereas the spectrum of 3,4-benzofluoranthene, consisting of five condensed aromatic rings, showed a C_2H^-/C_2^- ratio of 2.20 (Tab. 4).

The SIMS spectra strongly depended on the pyrolysis and the post-pyrolysis heat-treatment temperature during syn-

Table 4, SIMS; C_2H^-/C_2^- ratio (peak area)

Sample	C_2H^-/C_2^- ratio	Sample	C_2H^-/C_2^- ratio
3,4-benzofluoranthene	2.20	CMK-3F(A)	0.70
		CMK-3F(B)	0.51
CMK-1F(A)	1.09	CMK-3F(C)	0.15
CMK-1F(B)	0.65	CMK-3F(D)	0.11
CMK-1F(C)	0.48	CMK-3F(E)	0.07
CMK-1F(D)	0.51	CMK-3Na(A)	0.74
CMK-1F(E)	0.06	CMK-3Na(B)	0.34
CMK-1F(F)	0.11	CMK-3Na(C)	0.24
CMK-1Na(A)	0.95	Rubber carbon black, N539	0.51
CMK-1Na(B)	0.58		
CMK-1Na(C)	0.18	Conductive carbon black, XC-72	0.21
CMK-1Na(D)	0.06		
CMK-1Na(E)	0.04	Graphite	0.25

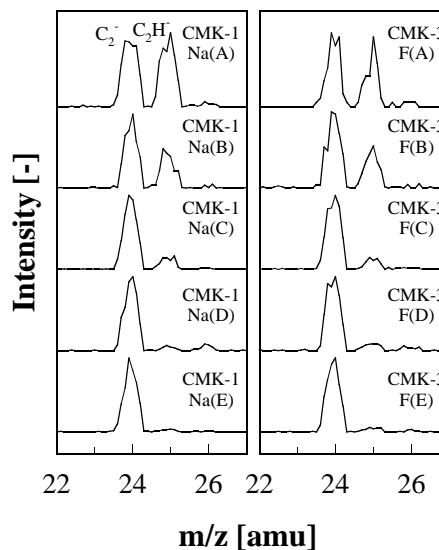


Fig. 6 SIMS spectra, negative ions, series CMK-1Na; normalised to the same height

thesis of the carbon sieves. As shown for the series CMK-1Na in Figure 6, the relative intensity of the C_2H^- peak (and therefore also the C_2H^-/C_2^- ratio) decreased with increasing temperature, indicating an increasing polyaromatic character of the surface. However, this decrease was limited to temperatures below approximately 1100 °C. A heat-treatment at higher temperatures only had a very limited effect on the C_2H^-/C_2^- ratio (Fig. 7). This observation indicates that at approximately 1100 °C a “maximum polyaromatic character” of the outer carbon sieve surface was reached.

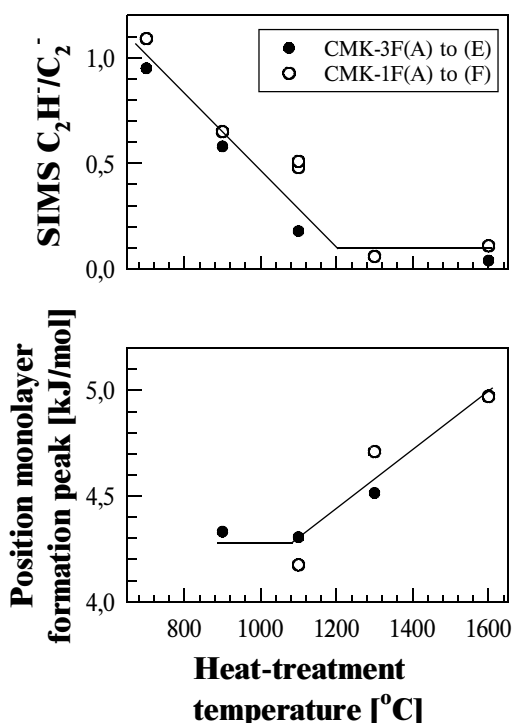


Fig. 7 SIMS C_2H^-/C_2^- ratio (measure for the polyaromatic character of the outer surface) and position of the monolayer formation peak (measure for the order of the mesopore surface) as a function of the heat-treatment temperature.

However, it is also possible that static SIMS fails to differentiate between samples with a very high polyaromatic character. It can be seen in Fig. 6 that for the carbon sieves heat-treated at temperatures above 1100 °C (e.g. samples CMK-1Na(D) and CMK-1Na(E)) the C_2H^- peak was very small. Thus, differences between different samples treated at temperatures above 1100 °C are not easy to detect.

It is interesting to note that the C_2H^-/C_2^- ratios of the carbon sieves heat-treated above 1100 °C were lower as compared to the poly-crystalline graphite and other compounds with a graphite-like surface such as rubber blacks and conductive carbon blacks (Tab. 4). Especially conductive carbon blacks have a high polyaromatic character which favours the electrical conductivity. This suggests that the outer surface of the heat-treated carbon sieves had an especially high polyaromatic character.

The temperature dependence of the C_2H^-/C_2^- ratio was very similar for the different series of carbon sieves. This confirms the conclusion from the ESCA study that the silica matrix had no or only very little influence on the polyaromatic character of the outer surface of the carbon sieves.

Comparison of the surface spectroscopic with nitrogen adsorption results

It was already mentioned, that the outer surface (probed by SIMS and ESCA) only represents a very small portion of the total surface of the carbon sieves. The largest portion

of the surface is present in narrow mesopores. The carbon sieves represent a special cases, where information on the graphitic order of the mesopore surface can be obtained from low-pressure nitrogen adsorption data [3].

On homogeneous surfaces the adsorption potentials of all adsorption sites are very similar. For very homogeneous surfaces samples each layer of adsorbed nitrogen is formed at the same relative pressure. Thus, in the corresponding isotherms (e.g. of exfoliated graphite) steps are observed which correspond to the successive formation of the various nitrogen layers [21]. The nitrogen adsorption isotherms of less homogeneous samples (e.g. graphitized carbon blacks) only show the monolayer formation step [22]. For more heterogeneous samples (e.g. non-graphitized carbon blacks) the monolayer step cannot be observed in the isotherm. However, even for many of these materials, a monolayer formation peak can be found in the corresponding adsorption potential distribution (APD). Formally, the APD may be regarded as a derivative of the adsorption isotherm (logarithmic scale of the relative pressure). The position of the monolayer formation peak depends on the graphitic order of the surface. For graphitized carbon blacks the monolayer formation peaks are located at adsorption potentials between 5 and 5.5 kJ/mol. With decreasing graphitic order, the monolayer formation peak is shifted to lower adsorption potentials [22]. The APD of porous carbons show pore filling peaks which interfere with the monolayer formation peak. However, because of the special pore structure of the carbon sieves, this was not the case for the samples studied in the present work [3]. It was therefore possible to obtain information on the graphitic order of their surface from the position of the monolayer formation peak in the APD. Since the mesopore surface is much larger as compared to the outer surface, the position of the monolayer formation peak depends essentially on the graphitic order of the mesopore surface. This allows the comparison of the graphitic order of the mesopore surface (as studied by low-pressure nitrogen adsorption) to the graphitic order of the outer surface (as studied by SIMS) and to the outer surface plus the region near to the outer surface (as studied by ESCA). For the carbon sieves synthesised at 700 °C no monolayer formation peak was observed, indicating a relatively low graphitic order of the surface. A monolayer formation peak at approximately 4.2 kJ/mol was found in the APD of the carbon sieves synthesised at 900 °C. With increasing synthesis temperatures (especially above 1100 °C) the monolayer peak was shifted to higher adsorption potentials (Fig. 7). This indicates an increasing graphitic order of the mesopore surface over the entire temperature range studied.

As mentioned above, the polyaromatic character of the outer surface plus the region near to the outer surface can be characterised by the FWHM of the C_1 ESCA peak. The FWHM decreased with increasing synthesis temperature, this decrease was more pronounced for temperatures above 1100 °C (Fig. 5). Thus, as it was the case for the mesopore

surface, the polyaromatic character of the surface studied by ESCA increased over the entire temperature range and especially above 1100 °C.

The comparison with the temperature dependence of the SIMS C_2H/C_2 ratio indicates that the development of the graphitic character on the outer surface was different. As already discussed above, the SIMS C_2H/C_2 ratio strongly decreased up to a temperature of 1100 °C and changed only little upon further heating (Fig. 7). As discussed above, this suggests that at 1100 °C the outer surface had already reached its "real" or detectable maximum polyaromatic character. The good correlation between the nitrogen adsorption and the ESCA results indicates that, at least for the sample studied here, some information on the chemistry of the internal mesopore surface can be drawn from the ESCA results. However, there were differences between the outer and the mesopore surface.

ESCA Oxygen spectra

The oxygen spectra were fitted to four peaks (Fig. 8): a peak for oxygen atoms with two bonds to carbon atoms (O_1 , C=O, BE = 531.1 eV), a peak for oxygen atoms with one bond to a carbon atom (O_2 , C-OH, BE = 532.8 eV) and to two peaks which could be due to adsorbed water and oxygen, respectively (O_3 and O_4 , BE = 535.1 and 537.6 eV) [13, 23].

As mentioned above, the silicon spectra indicated the presence of non-dissolved silicates on the carbon sieve surface. The BE of oxygen atoms in silicates is approximately 532.0 eV [24]. These oxygen atoms will therefore contribute to the O_2 peak. This contribution can be estimated by calculating the oxygen concentration in silica. Assuming that all silicon atoms are present in silica (no organic silicon compounds, as confirmed by the silicon spectra) and that all silicon atoms are bonded to two oxygen atoms the

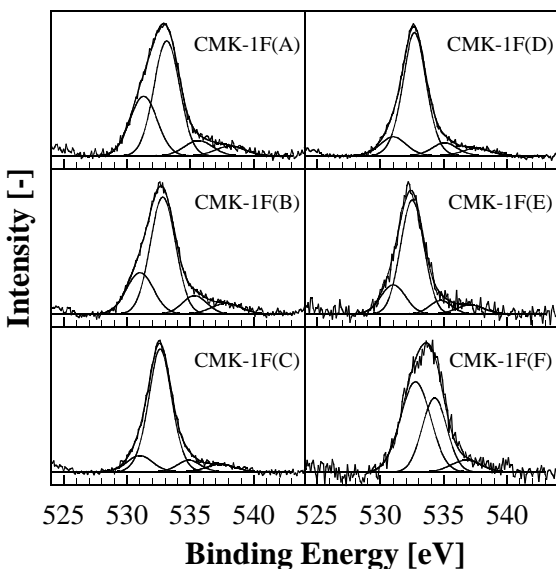


Fig. 8 Oxygen 1s spectra, series CMK-1F, normalised to the same height

Table 5, ESCA oxygen spectra; peak area

Sample	Relative peak area [%]				
	O_1 C=O	O_2 C-OH, SI-O	O_2^a C-OH	O_3 H_2O_{ads} / O_{ads}	O_4
CMK-1F(A)	31	56	46	8	5
CMK-1F(B)	23	61	41	9	7
CMK-1F(C)	11	75	28	7	5
CMK-1F(D)	13	74	46	8	6
CMK-1F(E)	18	68	-	8	6
CMK-1F(F)	-	55	30	37	7
CMK-1Na(A)	32	57	57	8	5
CMK-1Na(B)	22	63	44	9	6
CMK-1Na(C)	-	72	2	10	2
CMK-1Na(D)	-	71	-	22	7
CMK-1Na(E)	5	76	76	16	3
CMK-3F(A)	30	57	57	8	5
CMK-3F(B)	19	66	41	9	7
CMK-3F(C)	14	71	31	6	9
CMK-3F(D)	15	66	38	14	5
CMK-3F(E)	-	-	-	-	-
CMK-3Na(A)	34	52	52	7	7
CMK-3Na(B)	20	64	44	9	7
CMK-3Na(C)	19	65	33	9	7

^a Estimated area of the O_2 peak due to oxygen atoms with one bond to carbon, equation 5

concentration of oxygen in silica is two times the concentration of silicon:

$$O_{\text{silica}} = 2 \cdot Si_{\text{total}} \quad (4)$$

where O_{silica} is the concentration of oxygen in silica and Si_{total} is the total concentration of silicon (Tab. 2). In order to obtain the contribution of "C-OH type" oxygen, the area corresponding to these oxygen atoms is then subtracted from the O_2 peak:

$$A(O_2, C-OH) \sim A(O_2, C-OH + SiO_2) - \frac{O_{\text{silica}}}{O_{\text{total}}} \quad (5)$$

where $A(O_2, C-OH)$ is the relative area of the O_2 peak due to C-OH groups, $A(O_2, C-OH + SiO_2)$ is the relative area of the O_2 peak (Tab. 5) and O_{total} is the total concentration of oxygen (Tab. 2). It should be mentioned that because of the low surface concentrations of silicon this estimation is a relatively rough approximation.

In all oxygen spectra the O_2 peak was more intense than the O_1 peak. This was also the case when the contribution of oxygen atoms in silicates was subtracted from the O_2 peak (Tab. 5). These data indicate that the surface concentra-

tion of C-OH type oxygen was higher than the concentration of C=O type oxygen.

Conclusions

The outer surface of the mesoporous carbon molecular sieves has a graphite-like, polyaromatic character, similar to carbon blacks or carbon fibres. Higher temperatures during pyrolysis or a post-pyrolysis heat-treatment increases the polyaromatic character considerably. The outer surface of carbon sieves heated to temperatures above 1100 °C has a more pronounced polyaromatic character as compared to polycrystalline graphite, rubber carbon blacks or conductive carbon blacks. Upon heat-treatment, the graphitic character of the mesopore surface also increases. The structure of the silicate matrix used for the synthesis of the mesoporous carbon has no influence on the polyaromatic character of the surface. During dissolution of the silicate matrix in hydrofluoric acid, organic fluorine compounds are formed on the surface of the carbon sieves. A maximum surface fluorine concentration of 0.8 atom % was observed. Carbon sieves formed in MCM-48 have a higher surface fluorine concentration as compared to mesoporous carbon sieves formed in SBA-15. Furthermore, small concentrations of non-dissolved silicates are present on the surface of the carbon sieves. Dissolution of the silica matrix in sodium hydroxide yields a less contaminated carbon sieve as compared to dissolution in hydrofluoric acid.

References

- [1] Ryoo R, Joo SH and Jun S. Synthesis of highly ordered carbon molecular sieves via template-mediated structural transformation. *J. Phys. Chem. B.* 1999; 103: 7743-7746.
- [2] Shin HJ, Ryoo R, Kruk M and Jaroniec M. Modification of SBA-15 pore connectivity by high-temperature calcination investigated by carbon inverse replication. *Chem. Commun.* 2001, 349 - 350.
- [3] Darmstadt H, Roy C, Kaliaguine S, Choi S and Ryoo R. Pore Structure and Graphitic Surface Order of Mesoporous Carbon Molecular Sieves by Low-Pressure Nitrogen adsorption. *Carbon 2001, International Conference on Carbon, Lexington, Kentucky, USA July 14-19, 2001.*
- [4] Jun S, Joo SH, Ryoo R, Kruk M, Jaroniec M, Liu Z, Ohsuma T and Terasaki O. Synthesis of New Nanoporous Carbon with Hexagonally Ordered Mesoporous Structure. *J. Am. Chem. Soc.* 2000; 43: 10712 - 10713
- [5] Ryoo R, Joo SH and Kim JM. Energetically Favored Formation of MCM-48 from Cationic-Neutral Surfactant Mixtures. *J. Phys. Chem. B.* 1999; 103: 7435-7440.
- [6] Kruk M, Jaroniec M, Ryoo R and Joo SH. Characterization of Ordered Mesoporous Carbons Synthesized Using MCM-48 Silicas as Templates. *J. Phys. Chem. B.* 2000; 104: 7960-7968.
- [7] Sherwood P.M.A., In Briggs D., Seah M.P. Editors. *Practical Surface Analysis by Auger and X-ray Photoelectron Spectroscopy*, Chichester, UK, John Wiley & Sons Ltd., 1983, pp. 445.
- [8] Darmstadt H, Sümchen L, Roland U, Roy C, Kaliaguine S and Adnot A. Surface versus Bulk Chemistry of Pyrolytic Carbon Blacks by SIMS and Raman Spectroscopy. *Surf. Interface Anal.* 1997; 25: 245-253.
- [9] Menéndez JA, Phillips J, Xia B and Radovic, LR. On the Modification and Characterization of Chemical Surface Properties of Activated Carbon: In the Search of Carbons with Stable Basic Properties. *Langmuir* 1996; 12: 4404-4410.
- [10] Wagner CD, Riggs WM., Davis LE, Moulder, JF and Muilenberg GE. In: *Handbook of X-Ray Photoelectron Spectroscopy*. Eden Prairie, MN, USA, Perkin-Elmer Corporation, 1979.
- [11] Nanse G, Papirer E, Fioux P, Moguet F and Tressaud A. Fluorination of carbon blacks: an X-ray photoelectron spectroscopy study: I. A literature review of XPS studies of fluorinated carbons. XPS investigation of some reference compounds. *Carbon* 1997; 35: 175-194.
- [12] Desimoni E, Casella GI, Morone A and Salvi AM. XPS Determination of Oxygen-containing Functional Groups on Carbon-fibre Surfaces and the Cleaning of These Surfaces. *Surf. Interface Anal.* 1990; 15: 627-634.
- [13] Xie Y and Sherwood PMA. X-ray Photoelectron Spectroscopic Studies of Carbon Fiber Surfaces. 11. Differences in the Surface Chemistry and Bulk Structure of Different Carbon Fibers Based on Poly(acrylonitrile) and Pitch and Comparison with Various Graphite Samples. *Chem. Mater.* 1990; 2: 293-298.
- [14] Gardella JA, Ferguson SA and Chin RL. $\pi^* \rightarrow \pi$ Shakeup Satellites for the Analysis of Structure and Bonding in Aromatic Polymers by X-Ray Photoelectron Spectroscopy. *Appl. Spectrosc.* 1986; 40: 224-232.
- [15] Darmstadt H, Roy C and Kaliaguine S. ESCA Characterization of Commercial Carbon Blacks and of Carbon Blacks from Vacuum Pyrolysis of Used Tires. *Carbon* 1994; 32: 1399-1406.
- [16] Barr TL and Yin M. Concerted x-ray photoelectron spectroscopy study of the character of select carbonaceous materials. *J. Vac. Sci. Technol. A* 1992; 10: 2788-2795.
- [17] Kelemen SR, Rose KD and Kwiatak PJ. Carbon aromaticity based on XPS Π to Π^* signal intensity. *Appl. Surf. Sci.* 1992; 64: 167-173.
- [18] Cheung TTP. X-ray photoemission of polynuclear aromatic carbon *J. Appl. Phys.* 1984; 55: 1388-1393.
- [19] Morita K, Murata A, Ishitani A, Muragana K, Ono T and Nakajima A. Characterization of commercially

available PAN (polyacrylonitrile)-based carbon fibers. *Pure Appl. Chem.* 1986; 58: 456-468.

- [20] Darmstadt H, Roy C, Kaliaguine S, Ting J-M and Alig RL. Surface Spectroscopic Analysis of Vapour Grown Carbon Fibres Prepared Under Various Conditions. *Carbon* 1998; 36: 1183-1190.
- [21] Thomy A and Duval X. Stepwise isotherms and phase transitions in physisorbed films. *Surf. Sci.* 1994; 299-300: 415-425.
- [22] Kruk M, Li ZJ, Jaroniec M and Betz WR. Nitrogen

adsorption study of surface properties of graphitized carbon blacks. *Langmuir* 1999; 15: 1435-1441.

- [23] Xie Y and Sherwood PMA. X-Ray Photoelectron-Spectroscopic Studies of Carbon Fiber Surfaces. Part IX: The Effect of Microwave Plasma Treatment on Carbon Fiber Surfaces. *Appl. Spectrosc.* 1989; 43: 1153-1158.
- [24] Barr TL. In: *Modern ESCA The Principles and Practice of X-Ray Photoelectron Spectroscopy*. Boca Raton, FL, USA, 1984, CRC Press, pp. 283.